Basketball Video Image Segmentation Using Neutrosophic Fuzzy C-means Clustering Algorithm

Chao Hong
Ministry of Sports, Xiamen Institute of Technology, Xiamen 361021, China
E-mail: hc_0727@163.com

Keywords: video segmentation, fuzzy C-means clustering, neutrosophic fuzzy C-means clustering, basketball video images

Received: March 18, 2024

Basketball video image segmentation is important in image processing and computer vision, which is significant for improving image quality and enhancing visual effects. However, traditional image segmentation algorithms still have challenges in dealing with noise and complex backgrounds. Research on basketball video image segmentation based on Neutrosophic fuzzy C-means clustering algorithm was conducted in this paper. Firstly, the video image segmentation algorithm was studied and analyzed. Secondly, the computational time was reduced to get better segmentation results by fuzzy C-mean clustering. The algorithm was carried out for basketball video image segmentation, which was compared and analyzed with the traditional segmentation algorithm. Results showed that the peak SNR values were 14.96, 14.81, and 14.57 in pretzel noise environment. The peak SNR results were 13.97, 12.87, and 12.06 in Gaussian noise environment. The algorithm has a significant advantage in both image segmentation performance. It improves the image quality and visual effect, which is an important reference for future image analysis and processing.

Povzetek: Algoritem za segmentacijo video slik v košarki uporablja gručenje Neutrosophic fuzzy C-means, kar izboljša kakovost slike in vizualne učinke ter zmanjša čas izračuna v primerjavi s tradicionalnimi metodami.

1 Introduction

Basketball is a fast-paced and highly competitive sport with a rich variety of dynamic images and emotional changes. The accurate video image segmentation is a challenge [1]. Traditional video image segmentation methods can hardly deal with the complex and dynamic scenes in basketball games [2]. The Fuzzy C-means Clustering (ZFC) algorithm is a classical clustering segmentation method that can manage images containing noise and fuzzy edges [3]. However, the classical clustering segmentation method depends on the initial value and may fall into local optimal solutions [4]. An important research topic in video image segmentation technology is to improve the stability and accuracy of the ZFC algorithm [5]. In this study, a basketball video image segmentation method using Neutrosophic Fuzzy C-means Clustering (ZZFC) algorithm is proposed. This method aims to optimize the initial value selection and adopt intelligent optimization strategies to improve the stability and accuracy of segmentation. In this study, ZZFC is innovatively applied to basketball video image segmentation. Meanwhile, two strategies, center updating and intelligent optimization, are adopted to effectively improve the stability and accuracy of clustering. This study is important in promoting basketball video image segmentation technology. Therefore, accurate and high-quality data support and important value can be supplied for subsequent game analysis and athlete performance evaluation.

The research includes five parts. The first part describes how video image segmentation technology promotes computer and information science with the rapid development of information technology. The second part is the related works, which elaborate on the current research and implementation of video image segmentation algorithms by numerous scholars. The third part is the video image segmentation technology using ZZFC. The first section focuses on video image segmentation algorithms, while the second section focuses on the video image segmentation algorithms under ZZFC. In the fourth part, the proposed algorithm is tested. The fifth part is a summary and outlook of this study.

2 Related works

In the current research, basketball video image segmentation is a hot topic. However, traditional image segmentation methods often do not achieve ideal results due to the complexity and diversity. Many scholars have studied video image segmentation techniques. Fiaz et al. proposed a network architecture called 4G video object segmentation. This architecture improved the video object segmentation by encoding video context to address the background interference and object appearance changes. The guided transfer embedding module was

used to keep long-term semantic information in this architecture, and the global instance matching module generated similar mappings. The experimental results showed that 4G video object segmentation performed well among 40 existing methods [6]. Cao et al. proposed a segmentation scheme with two branches. The attention mechanism was first used to highlight features related to objects. Meanwhile, a designed attention residual convolution was used to capture the long and short-term temporal information of objects under redundant video frame interference. The segmented target was obtained using global thresholding and noise region removal methods based on the fusion results of the two branches. The experimental results demonstrated the competitive performance of the scheme [7]. Zhang et al. proposed a new method for monitoring video motion segmentation based on a progressive spatiotemporal tunnel flow model. A cyclic progressive spatiotemporal tunnel was established by gradually sampling pixels, and then it was unfolded to form a spatiotemporal tunnel unfolding map. Finally, the monitoring video motion segments were segmented based on this model. Results showed that this method was superior to existing methods in time consumption [8]. Zhu et al. proposed an algorithm for non-specific sperm aggregates. This algorithm created a grid model that was proportional to the sperm head size to segment non-specific aggregation areas. Meanwhile, multi-scale edge functions and new energy functions were designed to achieve sperm head segmentation. The research results indicated that this method achieved precise segmentation of sperm, outperforming the level set methods. The sperm concentration and vitality were calculated in real-time during sperm tracking [9]. Wang et al. proposed a feature reconstruction-based method for human portrait video segmentation. This method introduced a soft communication network that promoted feature reconstruction in an unsupervised manner by gently allocating the displacement probability of each pixel. More reliable segmentation results could be obtained by mining reconstructed features. The research results indicated the effectiveness of the method [10].

The ZZFC algorithm is a novel method for basketball video image segmentation, showing better advantages. Many scholars have conducted extensive research on it. Yang et al. proposed a fuzzy C-means algorithm that simultaneously handled noise and uncertainty issues in MRI images of human brain. Noise robust intuitionistic fuzzy sets were introduced to better handle images with noise. The research results indicated that the algorithm demonstrated effectiveness and superiority in many MRI experiments of human brain [11]. Z Dong et al. proposed a cold damage area segmentation algorithm using improved k-means clustering for detecting tomato frost damage. The research results indicated that the algorithm performed well in segmenting cold damaged areas in fluorescence imaging with yellow cold spots. The average matching rate and average error rate were better than the traditional methods [12]. K G Dhal et al. proposed a fuzzy clustering technique that combined rough set-based global, random attraction, and local search strategies to deal with image segmentation. The research results indicated that this technology outperformed various natural inspired algorithms in accuracy and segmentation output quality [13]. Bas et al. proposed a fuzzy inference system using Gustafson Kessel clustering algorithm. A fuzzy regression function method was used instead of rule base operation. This new method recognized ellipsoidal clustering without traditional limitations. The research results indicated that the fuzzy inference system using this clustering algorithm significantly improved predictive performance [14]. Li et al. proposed a spectral clustering algorithm using fuzzy similarity. The fuzzy similarity measurement was used to obtain the similarity between data points and anchor points, and then the similarity matrix was obtained. Results showed that the proposed algorithm had better classification performance for hyperspectral remote sensing images, with a 2% increase in kappa coefficient compared to traditional algorithms [15]. The summary of relevant research is shown in Table 1.

Table1: Summary table of related research

Method	Data set	Key findings	Limitations
M Fiaz et al.	DAVIS2016, DAVIS2017 and YouTube VOS	Has excellent image segmentation performance	Low efficiency
Y Cao et al.	DAVIS2016 and CDnet2014	Performed well in long video segmentation tasks	It is difficult to segment small object targets from videos with occlusion
Y Zhang et al.	8 real monitoring scenarios	Less time consumption	Lack of motion classification for motion segments
R Zhu et al.	Real sperm samples	Accurate segmentation of non-specific aggregation regions has been achieved	High demand for image quality
Y Wang et al.	DAVIS2016 and CDnet2014	Suitable for scenarios with significant posture changes	Low efficiency

		and severe occlusion	
Z Yang et al.	Brain Web	Combined with local spatial information, less affected by noise	Computational complexity
Z Dong et al.	Fluorescence images of tomato seedling leaves collected	The average matching rate of the image is relatively high	Poor processing effect for complex scenes
K Li et al.	Synthetic data and real word hyperspectral imaging dataset	Simple calculation, suitable for large-scale data classification such as hyperspectral remote sensing images	Poor stability

In summary, the existing advanced basketball video image segmentation methods have made great progress. However, there are still problems such as high computational complexity, high requirements for image quality, poor performance in complex scene processing, and poor stability. Therefore, this study proposes a basketball video image segmentation method based on the ZZFC algorithm. Specifically, the image segmentation method using the ZZFC introduces the Neutrosophic fuzzy theory to better handle uncertainty in images. Then the Neutrosophic fuzzy theory is combined with the C-means clustering algorithm to achieve more accurate image segmentation. As a result, image segmentation and noise can be handled effectively to preserve important features of the image. However, this method still has certain shortcomings, such as high computational complexity and difficulties in large-scale image processing. Therefore, the proposed methods still need to be improved and optimized to provide important directions and basis for future research.

3 Video image segmentation algorithm using neutrosophic fuzzy C-means clustering algorithm

Video image segmentation algorithms focus on image segmentation in video streams to improve image processing efficiency and accuracy. On this basis, the ZZFC algorithm is introduced to further improve the accuracy of image segmentation. The ZZFC algorithm can significantly reduce the impact of errors in image segmentation with the high adaptability to fuzziness and noise. This algorithm not only promotes the development of efficient video processing technology, but also provides new theoretical and application foundations for innovative exploration of image segmentation technology. It is hoped to provide new evidence and explore new perspectives for researchers in deep learning and machine vision.

3.1 Basketball video processing based on image segmentation algorithm

Video image segmentation, as a key technology in computer vision, has expanded the research space in multiple scientific fields such as modern image processing, machine learning, and artificial intelligence [16]. This technology analyzes the pixel population within a video frame to determine the object or scene it belongs to, thereby achieving precise analysis and understanding of video content. Video image segmentation algorithms rapidly evolve with the development of the combination of deep learning and image segmentation. The development of this method helps to improve video processing efficiency and accuracy. The video image segmentation algorithm is shown in Figure 1.

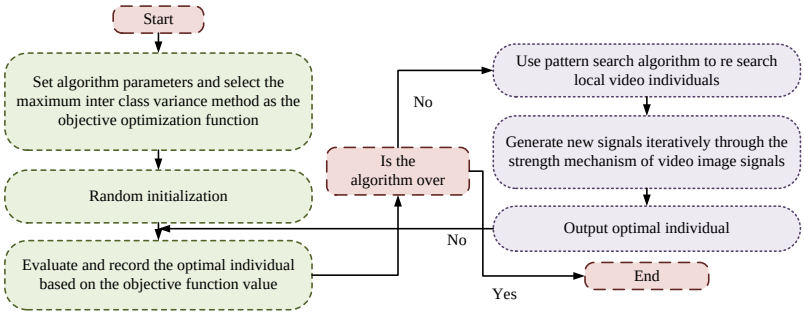

Figure 1: Video image segmentation algorithm

The algorithm consists of three main parts: preprocessing, segmentation, and post-processing [17]. In the preprocessing, video images are optimized through filtering, noise suppression, and other methods to

improve the accuracy of subsequent segmentation. The segmentation is the core of the algorithm, which distinguishes foreground objects and background scenes in the image. The segmentation usually relies on a generator network to achieve pixel level fine segmentation. In the post-processing, operations such as edge smoothing and hole filling are performed to improve the visual representation of the segmentation results. The frame difference method extracts the image background of the video motion target detection system, as calculated in equation (1).

$$\Delta I_t(x,y) = \left| I(x,y,t) - I(x,y,t-1) \right| \quad (1)$$

In equation (1), $I(x,y,t)$ represents the grayscale of the pixel with coordinate (x,y) in frame t of the video. $I(x,y,t-1)$ represents the grayscale of the pixel with (x,y) in $t-1$ of the video. $\Delta I_t(x,y)$ is the difference between the grayscale of $I(x,y,t)$ and $I(x,y,t-1)$. When the algorithm detects that the foreground target has voids inside the object and there is stretching distortion in the motion direction of the object, its mathematical expression is shown in equation (2).

$$D_t(x,y) = \begin{cases} 1, \left|\Delta I_t(x,y)\right| \geq \alpha \\ 0, \left|\Delta I_t(x,y)\right| < \alpha \end{cases} \quad (2)$$

In equation (2), α represents the threshold for restricting $\Delta I_t(x,y)$, and D_t represents the background for obtaining frame t. The formula for calculating the difference between the three frames is shown in equation (3) for three consecutive frames of video images.

$$\Delta I_t(x,y) = \left| I(x,y,t) - I(x,y,t-1) \right| \otimes \left| I(x,y,t) - I(x,y,t-1) \right| \quad (3)$$

In equation (3), when the $\Delta I_t(x,y)$ value in the area of frame t image is small, the possibility of its background is greater. When the $\Delta I_t(x,y)$ value in the field is high, foreground moving targets likelihood is higher. The calculation formula for the binary image $W_t(x,y)$ of its three-frame difference is shown in equation (4).

$$W_t(x,y) = \begin{cases} 1, \left|\Delta I_t(x,y)\right| \geq \alpha \\ 0, \left|\Delta I_t(x,y)\right| < \alpha \end{cases} \quad (4)$$

In equation (4), α represents the threshold introduced to restrict $\Delta I_t(x,y)$. In image segmentation, noise that affects image quality is easily generated, so it is necessary to preprocess video images. The video preprocessing combining reinforcement learning methods is shown in Figure 2.

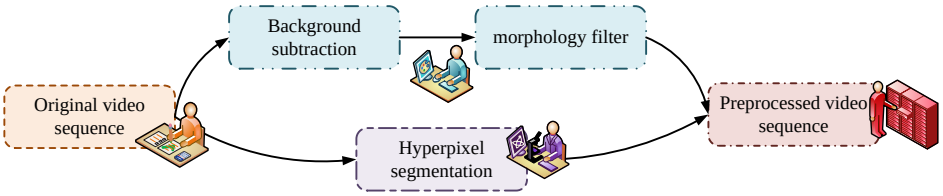

Figure 2: Video preprocessing process combining reinforcement learning methods

Video preprocessing is a key step in video image segmentation algorithms, aiming at optimizing the input video data to improve segmentation performance [18]. The preprocessing process first involves the collection and decoding of video frames, converting the raw data into a form that can be processed by the computer. The preprocessing processes are together constituted to provide higher quality input data for subsequent video image segmentation. The low-pass filtering method is used to convolve the impulse response functions of images and filters in the spatial domain. The mathematical expression of the convolution is shown in equation (5).

$$g(u,v) = \sum_x \sum_y f(x,y) H(u-x+1, v-y+1) \quad (5)$$

In equation (5), $f(x,y)$ represents the image. $H(x,y)$ represents the impulse response function of the filter. The motion video segmentation algorithm using global motion constraints and Markov random fields is a complex and effective image processing method. The video segmentation algorithm is shown in Figure 3.

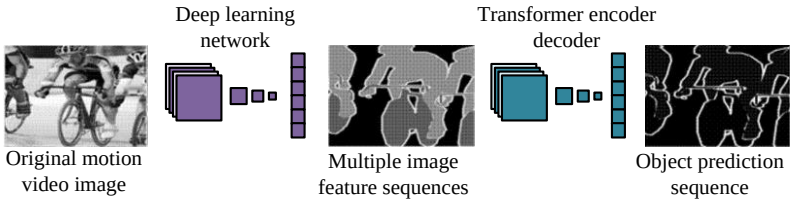

Figure 3: A video segmentation algorithm using global motion constraints and markov random fields

First, the video segmentation algorithm using global motion constraints and Markov random fields preprocesses the video frames using global motion constraints. Then local motion information of foreground objects is obtained by estimating and removing global motion. Next, Markov random field model is established, which combines the spatial relationships between pixels and time series information to achieve video frame segmentation. The calculation formula for setting the coordinate points (x, y) and $(x^{'}, y^{'})$ corresponding to the current frame and the previous frame is shown in equation (6).

$$x^{'} = \frac{m_0 x + m_1 y + m_2}{m_6 x + m_7 y + 1}, y^{'} = \frac{m_3 x + m_4 y + m_5}{m_6 x + m_7 y + 1} \quad (6)$$

In equation (6), m represents global motion parameters. m_t represents the motion model parameters calculated at frame t. The mathematical expression is shown in equation (7).

$$MV^{res}(x, y, t) = MV(x, y, t) - MV(x, y, m_t) \quad (7)$$

In equation (7), $MV^{res}(x, y, t)$ represents the final MV calculation result. The calculation formula for clustering the motion vectors is shown in equation (8).

$$MV_{cent} = \sum_j W_j MV_j^{res} / \sum_j W_j \quad (8)$$

In equation (8), MV_j^{res} represents the motion vector of each individual, and $W_j = \exp(-D_{MAXj})$ represents the weights in the domain. The video image segmentation algorithm accurately segments complex basketball game scenes to further provide accurate analysis of motion trajectories, speeds, and behavioral patterns. This algorithm plays a key role in promoting basketball training, game strategy development, and viewing experience.

3.2 Video image segmentation using neutrosophic fuzzy C-means clustering algorithm

The quality of video image segmentation directly affects the application of video [19]. The traditional method is prone to problems such as initial value selection, noise influence, and extreme value sensitivity when processing complex video images, as shown in Figure 4. These challenges can be solved by introducing fuzzy logic and Neutrosophic theory.

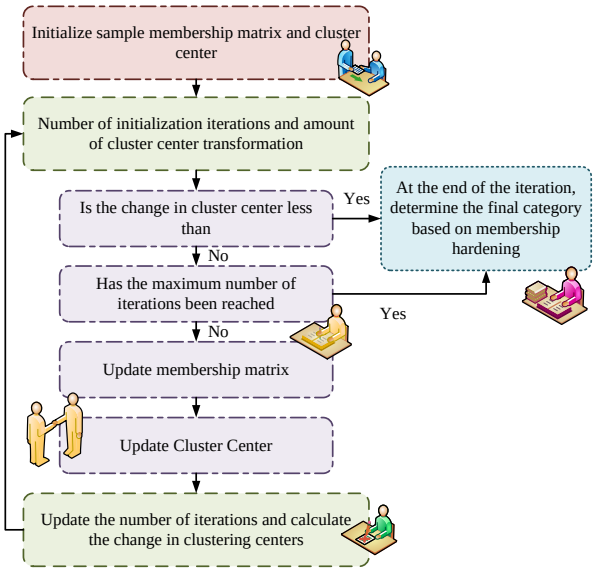

Figure 4: Fuzzy C-means clustering algorithm

The ZFC algorithm allows data points to belong to multiple cluster centers by hard C-means clustering. The membership degree of each cluster is a continuous value between 0 and 1. The ZFC algorithm adjusts the center and membership alternately until the end condition is met or the preset number of iterations is reached. The fuzzy clustering method is applied in image segmentation problems. Meanwhile, the mean clustering method with parameter z is introduced. The mathematical expression of the objective function is shown in equation (9).

$$J(U,V)=\sum_{i=1}^{N}\sum_{j=1}^{c}u_{ij}^{m}d^{2}(x_i,v_j) \qquad (9)$$

In equation (9), m represents the fuzzy parameter, with a value of 2. The membership of u_{ij} in $U=\left[u_{ij}\right]$ represents the degree to which each data point x_n belongs to different categories, with a value range of $[0,1]$. The total membership degree of each sample set is 1, so the range of U is shown in equation (10).

$$U\in\left\{u_{ij}\in[0,1]\left|\sum_{j=1}^{c}u_{ij}=1,\forall k and 0<\sum_{i=1}^{N}u_{ij}<N,\forall i\right.\right\} \quad (10)$$

In equation (10), u_{ij} represents updating the cluster center. The ZZFC algorithm partitions the elements in the dataset into various clusters, while allowing them to belong to multiple clusters [20]. The ZZFC algorithm is shown in Figure 5.

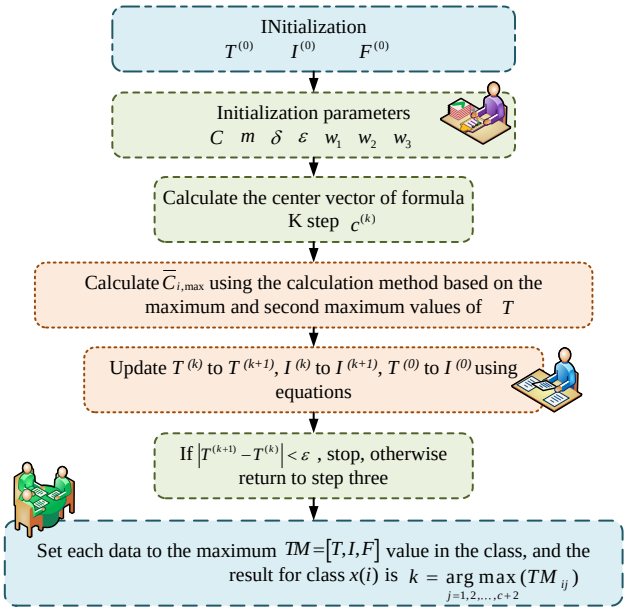

Figure 5: Neutrosophic fuzzy C-means clustering algorithm

The membership in this algorithm is calculated by fuzzy logic, and the result can better reflect the fuzziness between data. The algorithm iteratively updates the membership of cluster centers and elements until the predetermined stopping conditions are reached. The objective function of the two closest determined clusters is simplified by only considering the maximum and second largest membership values. Meanwhile, the computational cost is reduced, but the clustering accuracy will not be reduced. The expression of its objective function is shown in equation (11).

$$\min J_m(U,I,F,V)=\sum_{i=1}^{n}\sum_{j=1}^{c}(w_1u_{ij})^{m}\left\|x_i-v_j\right\|^{2}+\sum_{i=1}^{u}(w_2I_i)^{m}\left\|x_i-\overline{v_{i,\max}}\right\|^{2}+\sum_{i=1}^{n}\delta^{2}(w_3F_i)^{m} \quad (11)$$

In equation (11), m is a constant. P_i and P_e represent the number of clusters with the highest and second highest values. The datasets for boundary areas and noise, $0<T_{ij}$, I_i , and $F_i<1$, the following equations are satisfied, as shown in equation (12).

$$\sum_{j=1}^{C}T_{ij}+I_i+F_i=1 \qquad (12)$$

In equation (12), T_i , T_{ij} , I_i , and F_i represent the membership that belongs to the determined cluster. The ZZFC video segmentation algorithm is an optimization method using fuzzy logic and C-means clustering, focusing on efficient segmentation of video content to obtain finer content structures. The ZZFC video segmentation algorithm is shown in Figure 6.

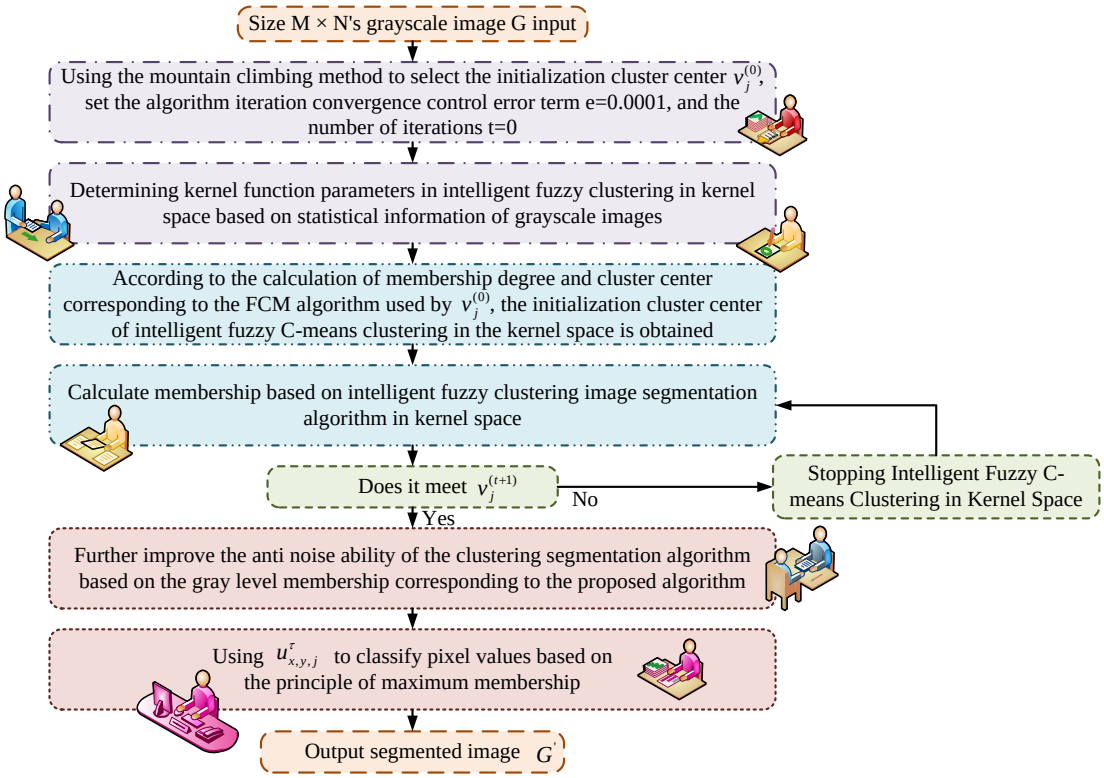

Figure 6: Neutrosophic fuzzy C-means clustering video segmentation

This algorithm compensates for the shortcomings of traditional ZFC algorithms in handling image noise and detail complexity by introducing Neutrosophic fuzzy logic. Firstly, the video frames are converted into a fuzzy set, and then C-means clustering processes the fuzzy set, forming multiple non-overlapping clusters. After processing the image information, the loss of the original image quality is calculated using the mean square error method, as shown in equation (13).

$$MSE = \frac{1}{mn}\sum_{i=0}^{m-1}\sum_{j=0}^{n-1}\left\|I(i,j)-K(i,j)\right\|^{2} \quad (13)$$

In equation (13), I and K represent two monochromatic graphs. The mathematical expression for its peak signal-to-noise ratio is shown in equation (14).

$$PSNR = 10\cdot\log_{10}\left(\frac{MAX_J^2}{MSE}\right) = 20\cdot\log_{10}\left(\frac{MAX_I}{\sqrt{MSE}}\right) \quad (14)$$

In equation (14), MAX_I represents the maximum value of image points color. The algorithm can achieve efficient recognition of inter frame coherence and video content while ensuring segmentation accuracy through iterative optimization.

4 Test analysis of video image segmentation algorithm using neutrosophic fuzzy C-means clustering algorithm

The study used the Potsdam dataset to verify the effectiveness and superiority of the segmentation performance of the ZZFC algorithm with the proposed local information constraints for segmentation of images [21]. The ZFC, FCM, and ZZFC algorithms were selected to have good noise immunity. The maximum iteration was set to 300, the weight of the criterion function was set to 1.5, the clusters were set to 8, the fuzzy factor was set to 2, the error was set to 0.001, and the classifications were set to 2. The hardware environment for testing and analysis included a computer with Intel Core i7-9700K processor with 32GB of RAM and 1TB SSD as hard disk. The experimental running environment windows XP with MATLAB 7.0 was chosen as the development platform. The programming environment was Python 3.8. OpenCV 4.5.1 was used for video image processing and Scikit-learn 0.24.1 library was used to implement the ZZFC algorithm. In addition, the NumPy 1.20.1 library was used for high performance scientific computing and data analysis, and the Matplotlib 3.3.4 library was used for image display and result plotting. The segmentation results of different algorithms for the figure and cotton images are shown in Figure 7.

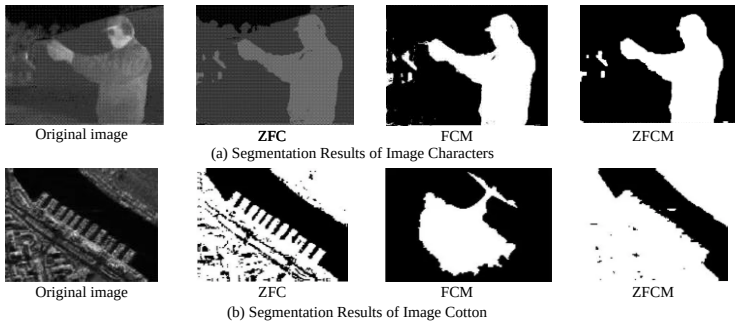

Figure 7: Segmentation results of different algorithms for character and cotton images

In Figure 7, the superior performance of the ZZFC algorithm in image detail segmentation was demonstrated, and its segmentation accuracy was also significantly improved. The ZZFC algorithm showed a more precise segmentation effect, with a significant reduction in misclassification in the segmentation experiment of character images in Figure 7 (a). The ZZFC algorithm had significantly overall evaluation performance better than ZFC and FCM algorithms. In Figure 7 (b), the ZZFC algorithm significantly improved the segmentation accuracy in details such as windows and stairs, with strong detail expressiveness. The performance of the ZZFC algorithm clearly surpassed the other two segmentation algorithms. The advantages of the ZZFC algorithm in image segmentation provided new ideas and methods for further research on image segmentation technology. The PSNR results of different algorithms are shown in Figure 8.

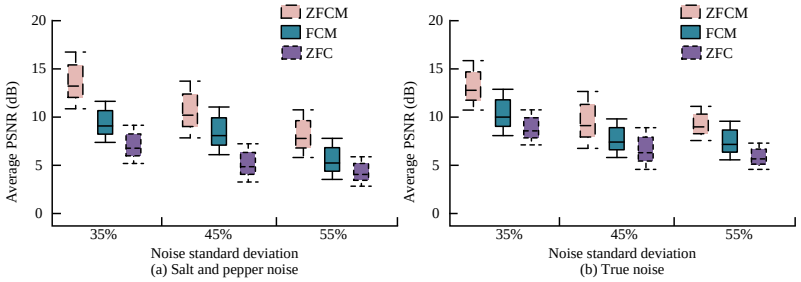

Figure 8: PSNR results of different algorithms under spicy salt noise interference

Figure 8 (a) shows the average PSNR performance of each algorithm. The PSNR values achieved by the ZZFC algorithm all showed the best performance when the noise standard deviation was set to 35, 45, and 55. The average PSNR improvement ratio of ZZFC compared to the FCM algorithm was 13.45%, 11.54%, and 9.19%, respectively, when the noise standard deviation was 35, 45, and 55. Similarly, the average PSNR improvement of ZZFC compared to ZFC algorithm was 21.94%, 21.74%, and 23.68%, respectively, when the noise standard deviation was 35, 45, and 55. In Figure 8 (b), the average PSNR performance of each algorithm is shown under real noise conditions. The ZZFC algorithm had the best PSNR values under various standard deviation conditions, indicating its excellent performance in image denoising. ZZFC significantly improved compared to the average PSNR of FCM and ZFC algorithms at noise standard deviations of 35, 45, and 55. The PSNR results of different algorithms under Gaussian noise interference are shown in Figure 9.

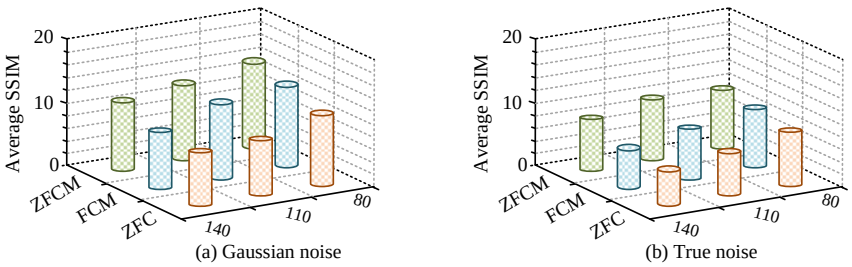

Figure 9: Different PSNR under gaussian noise interference

In Figure 9 (a), the SSIM values obtained by the ZZFC algorithm were better when the noise standard deviation was set to 80, 110, and 140. The improvement rates of ZZFC reached 7.12%, 12.83%, and 18.29%, respectively, compared with the average SSIM of the FCM algorithm at noise standard deviations of 80, 110, and 140. The improvement of ZZFC was more significant, with 43.23%, 45.19%, and 41.18%, respectively, compared with the average SSIM of the ZFC algorithm under the same noise standard deviation. In Figure 9 (b), the SSIM values of the ZZFC algorithm were all optimal when the noise standard deviations were 80, 110, and 140. This meant that the denoised image had a higher structural similarity with the original image. The improvement percentages of ZZFC algorithm were 11.23%, 18.27%, 21.09%, and 39.72%, 37.84%, and 46.32%, respectively, compared with the average SSIM of FCM and ZFC algorithms at noise standard deviations of 80, 110, and 140. The ZZFC algorithm had the best denoising ability, followed by the FCM algorithm, which had a relatively weak denoising effect. The comparison of PSNR results for segmentation performance under different algorithms against salt and pepper and Gaussian noise is shown in Table 2.

Table 2: Comparison of PSNR results for segmentation performance of different algorithms against spicy salt and gaussian noise

Salt and pepper noise	FCM	ZFC	ZZFC
35%	11.15	13.96	14.96*
45%	9.07	14.25	14.81*
55%	7.79	13.88	14.57*
Gaussian noise	FCM	ZFC	ZZFC
80	12.08	12.98	13.97*
110	11.63	12.11	12.87*
140	9.76	11.52	12.06*

Note: * indicates a significant difference (P<0.05) between the ZZFC and FCM algorithms, while # indicates a significant difference (P<0.05) between the ZZFC and ZFC algorithms.

According to Table 2, the ZZFC algorithm achieved the highest PSNR values at 35%, 45%, and 55% noise levels under salt and pepper noise, which were 14.96, 14.81, and 14.57, respectively. There was a significant difference (P<0.05) between the ZZFC and FCM algorithms. Under Gaussian noise, the ZZFC algorithm also showed the best PSNR results at noise of 80, 110, and 140, with values of 13.97, 12.87, and 12.06, respectively. There was a significant difference (P<0.05) between the ZZFC and FCM algorithms. The ZZFC algorithm showed superiority in image segmentation performance in both environments. In Chapter 4, experiments were conducted on simple scene video segmentation using Tennis and Stefan video sequences to verify the algorithmic effectiveness. Tennis had relatively small background changes, while Stefan had relatively large background changes and noise. Figure 10 shows the average accuracy, recall, and F-value curves of the segmentation results.

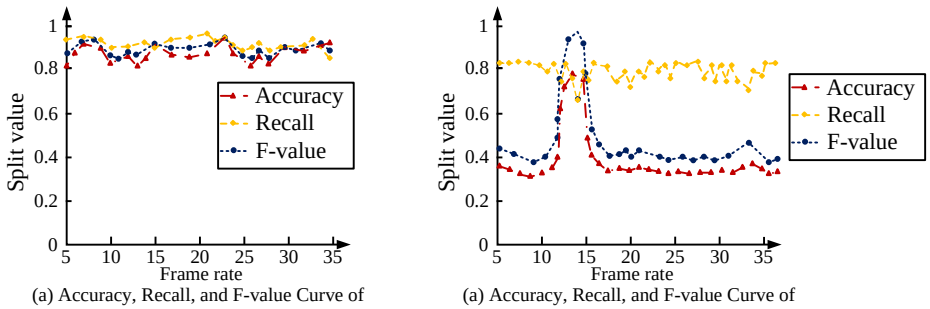

(a) Accuracy, Recall, and F-value Curve of Tennis Video Sequence Segmentation Results

(a) Accuracy, Recall, and F-value Curve of Stefan Video Sequence Segmentation Results

Figure 10: Average accuracy, recall, and F-value curves of segmentation results using different algorithms

In Figure 10, the accuracy of Tennis video sequences was generally high, while the accuracy of

Stefan video sequences slightly declined. In Figure 10 (a), the fluctuation of the segmentation curve was relatively small, with accuracy, F-measure, and recovery fluctuating between 0.8 and 0.97. In Figure 10 (b), Stefan's segmentation results decreased compared to the Tennis video sequence, but its accuracy only decreased by 4.6% in more complex scenes. The image background of the Tennis video sequence was relatively stable, and the overall effect of background removal was excellent. However, the video segmentation results of ZZFC algorithm showed higher recovery rate, accuracy, and F-measure compared with the segmentation results of Stefan video sequences. The comparison of accuracy, recall, and F-value results of the ZZFC algorithm under the Tennis and Stefan sequences is shown in Table 3.

Table 3: Comparison of accuracy, recall, and F-value results of ZZFC algorithm under tennis and stefan sequences

Video Sequence	Algorithm	Accuracy	Recall	F value
Tennis	ZFC	0.81	0.79	0.83
	ZFC	0.91	0.84	0.88
	ZZFC	0.96	0.92	0.93
Stefan	ZFC	0.37	0.29	0.93
	ZFC	0.23	0.26	0.92
	ZZFC	0.18	0.15	0.97

Table 3 shows the comparison results of ZZFC, ZFC, and FCM algorithms in terms of accuracy, recall, and F-value. The ZZFC algorithm outperformed the other two algorithms in all aspects in the video sequence, with an accuracy of 0.96, a recall of 0.92, and an F-value of 0.93. Although the accuracy and recall of the ZZFC algorithm were 0.18 and 0.15, respectively, lower than ZFC and FCM algorithms for the Stefan sequence. The F-value was 0.97, still better than the other two algorithms. The ZZFC algorithm had higher performance in comprehensive evaluation. The parallel computing and preprocessing of video images could be considered to improve the computational efficiency for the shortcomings of the proposed algorithm. Otherwise, the algorithm parameters were set reasonably and adjusted according to different situations to improve the algorithmic performance. In addition, hardware acceleration such as FPGA can be utilized to significantly improve the algorithmic running speed and real-time processing capabilities.

5 Discussion

This study proposes a basketball video image segmentation study using the ZZFC algorithm. The experimental results showed that the average PSNR value of the ZZFC algorithm performed best when the noise standard deviation was set to 35, 45, and 55 in a salt and pepper noise environment. The average PSNR improvement ratio of ZZFC under the same noise standard deviation was 13.45%, 11.54%, and 9.19%, respectively, compared with the FCM algorithm. The average PSNR improvement ratio of ZZFC under the same noise standard deviation was 21.94%, 21.74%, and 23.68%, respectively, compared with the ZFC algorithm. The average PSNR value of the ZZFC algorithm was still optimal under real noise conditions, proving its excellent performance in image denoising. When the noise standard deviation was set to 80, 110, and 140, the SSIM value of the ZZFC algorithm was better than other algorithms, indicating that the denoised image had a higher structural similarity with the original image. The image segmentation efficiency of our research algorithm was higher compared with references [6] and [10]. This is because our study combines the image segmentation method of neutral fuzzy mean clustering algorithm and neutral fuzzy theory, which can better handle the uncertainty of images. The C-means clustering algorithm was introduced to achieve more accurate image segmentation. The computational difficulty of the algorithm in this study was smaller compared with reference [11]. Similar to references [7] and [12], the algorithm in this study had poor image segmentation performance in complex backgrounds. In the future, further exploration can be made to combine it with other image processing techniques to improve the algorithm's image segmentation performance and efficiency.

6 Conclusion

Basketball video image segmentation is used in sports video analysis, event detection, and athlete tracking. However, the task of image segmentation becomes extremely difficult due to the complexity of basketball game scenes. These scenes involve multiple moving athletes, basketball, and environmental backgrounds. Traditional image segmentation algorithms often struggle to accurately segment athletes, basketball, and the background effectively, especially in noisy environments. Therefore, this study proposed a basketball video image segmentation study using the ZZFC algorithm to deal with this challenge. The proposed basketball video image segmentation method had important practical significance for improving image quality and visual effects. This study shows excellent performance in denoising and image similarity. However, the proposed algorithm still has poor

efficiency and stability when dealing with large-scale data or complex scenes. These challenges may affect the application effect of the algorithm in actual basketball video image segmentation. Therefore, further exploration should be conducted to combine the ZZFC algorithm with other image processing techniques to improve the depth and breadth of image processing in future research. The monitoring system can more accurately detect and track various events and dynamics in basketball games by applying the proposed algorithm to monitoring and sports analysis. Therefore, accuracy and efficiency can be improved. The proposed algorithm can also be used to analyze and identify various actions and events in basketball games. This can help teams and coaches to have a deeper understanding of the game situation and player performance, thereby formulating more scientific tactical strategies. However, the proposed basketball video image segmentation method may involve infringement of privacy information. Therefore, fuzzification can be used when using algorithms to protect privacy.

Reference

[1] F. Yu, Y. Zhu, X. Qin, Y. Xin, D. Yang, and T. Xu, "A multi-class COVID-19 segmentation network with pyramid attention and edge loss in CT images," IET Image Processing, vol. 15, no. 11, pp. 2604-2613, 2021. https://doi.org/10.1049/ipr2.12249

[2] W. Sprague, and E. R. Azar, "Integrating acceleration signal processing and image segmentation for condition assessment of asphalt roads," Canadian Journal of Civil Engineering, vol. 49, no. 6, pp. 1095-1107, 2022. https://doi.org/10.1139/cjce-2021-0116

[3] H. Yin, N. Chen, L. Yang, and J. Wan, "Pop-net: A self-growth network for popping out the salient object in videos," IET Computer Vision, vol. 15, no. 5, pp. 334-345, 2021. https://doi.org/10.1049/cvi2.12032

[4] H. Li, and J. Wang, "CAPKM++2.0: An upgraded version of the collaborative annealing power k -means++ clustering algorithm," Knowledge-Based Systems, vol. 262, no. 28, pp. 2-14, 2023. https://doi.org/10.1016/J.KNOSYS.2022.110241

[5] X. M. Long, Y. J. Chen, and J. Zhou, "Development of AR experiment on electric-thermal effect by open framework with simulation-based asset and user-defined input," Artificial Intelligence and Applications, vol. 1, no. 1, pp. 52-57, 2023. https://doi.org/10.47852/bonviewAIA2202359

[6] M. Fiaz, M. Z. Zaheer, A. Mahmood, L. Seung-Ik, and J. Soonki, "4G-VOS: video object segmentation using guided context embedding," Knowledge-Based Systems, vol. 231, no. 14, pp. 2-14, 2021. https://doi.org/10.1016/j.knosys.2021.107401

[7] Y. Cao, L. Sun, C. Han, and G. Jian, "Attention-based video object segmentation algorithm," IET Image Processing, vol. 15, no. 8, pp. 1668-1678, 2021. https://doi.org/10.1049/ipr2.12135

[8] Y. Zhang, W. Li, and Yang. P, "Surveillance video motion segmentation based on the progressive spatio-temporal tunnel flow model," Electronics Letters, vol. 57, no. 13, pp. 12-186, 2021. https://doi.org/10.1049/ell2.12186

[9] R. Zhu, Y. Cui, E. Hou, and J. Huang, "Efficient detection and robust tracking of spermatozoa in microscopic video," IET Image Processing, vol. 15, no. 13, pp. 3200-3210, 2021. https://doi.org/10.1049/ipr2.12316

[10] Y. Wang, L. Wang, W. Zhang, F. Yang, and H. Lu, "Temporal consistent portrait video segmentation," Pattern Recognition, vol. 120, no. 2, pp. 108-143, 2021. https://doi.org/10.1016/j.patcog.2021.108143

[11] Z. Yang, P. Xu, Y. Yang, and B. Kang, "Noise robust intuitionistic fuzzy C-means clustering algorithm incorporating local information," IET Image Processing, vol. 15, no. 3, pp. 805-817, 2021. https://doi.org/10.1049/ipr2.12064

[12] Z. Dong, Y. Men, Z. Li, Z. Liu, and J. Ji, "Chilling injury segmentation of tomato leaves based on fluorescence images and improved k-means clustering," Transactions of the ASABE, vol. 64, no. 1, pp. 13-22, 2021. https://doi.org/10.13031/trans.13212

[13] K. G. Dhal, A. Das, S. Ray, and J. Galvez, "Randomly attracted rough firefly algorithm for histogram based fuzzy image clustering," Knowledge-Based Systems, vol. 216, no. 15, pp. 2-20, 2021. https://doi.org/10.1016/j.knosys.2021.106814

[14] E. Bas, and E. Egrioglu, "A fuzzy regression functions approach based on Gustafson-Kessel clustering algorithm," Information Sciences, vol. 592, no. 5, pp. 206-214, 2022. https://doi.org/10.1016/j.ins.2022.01.057

[15] K. Li, J. Xu, T. Zhao, and Z. Liu, "A fuzzy spectral clustering algorithm for hyperspectral image classification," IET Image Processing, vol. 15, no. 12, pp. 2810-2817, 2021. https://doi.org/10.1049/ipr2.12266

[16] Z. Zhao, S. Zhao, and J. Shen, "Real-Time and light-weighted unsupervised video object segmentation network," Pattern Recognition, vol. 120, no. 4, pp. 110-120, 2021. https://doi.org/10.1016/j.patcog.2021.108120

[17] Z. Zhao, Y. Jin, J. Chen, B. Lu, C-F. Ng, Y-H. Liu, Q. Dou, and P. Heng, "Anchor-guided online meta-adaptation for fast one-shot instrument segmentation from robotic surgical videos,"

Medical Image Analysis, vol. 74, no. 2, pp. 102-113, 2021. https://doi.org/10.1016/j.media.2021.102240

[18] J. Zhang, L. Zhu, L. Yao, X. Ding, D. Chen, H. Wu, Z. Lu, W. Zhou, L. Zhang, P. An, B. Xu, W. Tan, S. Hu, F. Cheng, and H. Yu, "Deep learning-based pancreas segmentation and station recognition system in EUS: development and validation of a useful training tool (with video) (vol 92, pg 874, 2020)," Gastrointestinal Endoscopy, vol. 93, no. 3, pp. 780-781, 2021. https://doi.org/10.1016/j.gie.2020.04.071

[19] T. Zhang, D. Li, Y. Cai, and Y. Xu, "Super-resolution reconstruction of noisy video image based on sparse," Informatica, vol. 43, no. 3, pp. 414-420, 2019. https://doi.org/10.31449/inf.v43i3.2916

[20] G. L. Franklin, E. P. Bacheladenski, D. C. B. Rodrigues, and A. C. S. Crippa, "Teaching video neuroImage: stop-motion chorea in PURA syndrome," Neurology, vol. 100, no. 10, pp. 492-493, 2023. https://doi.org/10.1212/WNL.0000000000201605

[21] F. Chen, H. Liu, Z. Zeng, X. Zhou, and X. Tan, "BES-Net: Boundary enhancing semantic context network for high-resolution image semantic segmentation," Remote Sensing, vol. 14, no. 7, pp. 1638-1638, 2022. https://doi.org/10.3390/rs14071638